

INCLUDING CORRELATED FAILURE MODES IN SEISMIC FRAGILITY ANALYSIS

Michael W. Salmon¹ and Andrew S. Whittaker²

¹ Research Engineer; Los Alamos National Laboratory, Los Alamos, New Mexico, USA

² Professor and Chair, Director MCEER; University at Buffalo, Buffalo, New York, USA

ABSTRACT

Seismic probabilistic risk assessment (SPRA) of commercial nuclear power plants and many non-nuclear industrial facilities typically consist of three major tasks, namely, 1) probabilistic seismic hazard assessment, 2) development of seismic fragilities, and 3) preparation of fault trees and event trees that model the systems interactions and failure sequences. The methodology for conducting these tasks is mature and has been successfully applied to a large percentage of the operating commercial nuclear power plants in the United States. It is common practice in SPRA for the fragility analyst to select several credible failure modes, and then to report the seismic capacity of the structure, system or component as being equal to the lowest computed capacity. It is much less common for the analyst to select Boolean combinations of related failure modes to report a more accurate fragility. A two-mode failure model is considered here to explore this issue and the sensitivity of the computed failure frequency to the correlation between the failure modes is investigated to illustrate the process and provide sample results. For this example, the error introduced into the computed frequency of failure is small, unless the medians of the fragility curves differ by less than 10% and are weakly correlated.

INTRODUCTION

The purpose of this paper is to present the results of a study that examines the error introduced into seismic probabilistic risk assessment when the fragility function of selected structures, systems and components is reported as the lowest computed failure mode as opposed to considering some Boolean combination of closely spaced failure modes. The method used to derive the fragility functions is not relevant for the purpose of this study.

Seismic fragility functions are needed for nuclear power plant risk studies. Kennedy and Ravindra (1984) define the seismic fragility of a structure, system or component as the conditional frequency of failure for a given value of the spectral response parameter (e.g., stress, moment, spectral acceleration). The seismic fragility for a structure, system, or component is frequently expressed in terms of capacity measured in terms of ground acceleration, A , and random variables, ε_R and ε_U :

$$A = \bar{A} \varepsilon_R \varepsilon_U \quad (1)$$

where \bar{A} is the median capacity, and ε_R and ε_U are random variables with unit medians, and the inherent randomness about the median and the uncertainty in the median, respectively. In this model, it is assumed that both ε_R and ε_U are lognormally distributed with logarithmic standard deviations, β_R and β_U , respectively. Peak ground acceleration has traditionally been used as ground motion parameter to measure capacity although other spectral quantities are likely better. Most often the fragility parameters

\bar{A} , β_R , and β_U are estimated using an intermediate random variable described as a factor of safety, F . The median factor of safety, \bar{F} , is directly related to the median capacity, \bar{A} , as:

$$\bar{F} = \bar{A} / A_{SSE} \quad (2)$$

where A_{SSE} is a ground motion parameter (e.g., peak ground acceleration or spectral acceleration at a user-specified period) corresponding to a level of earthquake shaking such as a Safe Shutdown Earthquake or a Ground Motion Response Spectrum. The logarithmic standard deviation of F and A are assumed to be identical. A typical fragility curve is shown in Figure 1 together with a point on the fragility curve that is defined as the High Confidence of Low Probability of Failure (HCLPF). The HCLPF represents the acceleration at which there is 95% confidence of less than about a 5% probability of failure, which translates to approximately a 1% probability of failure based on the mean fragility curve.

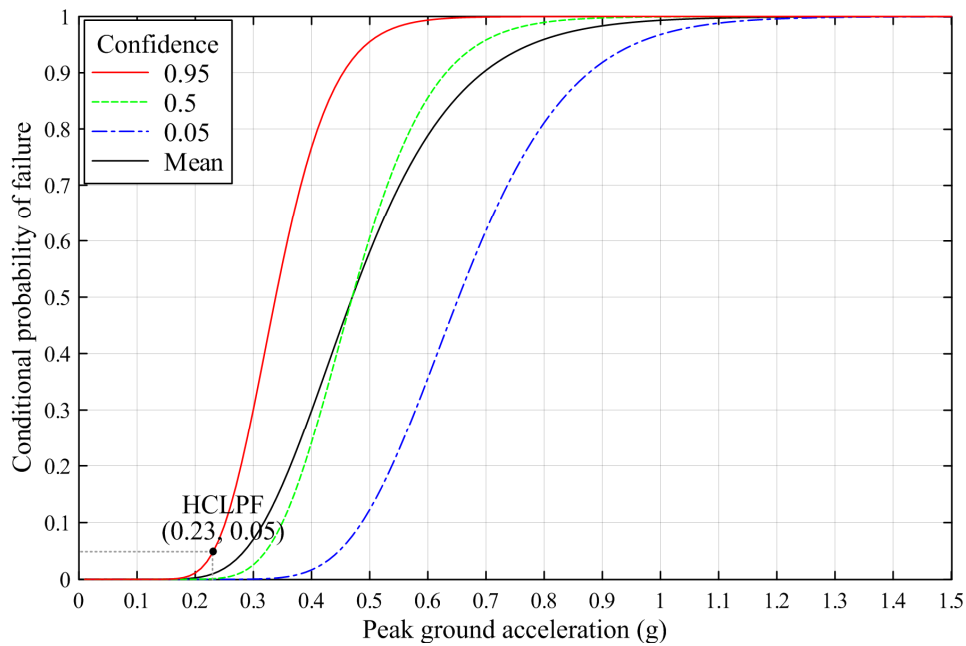


Figure 1. Sample fragility function for $\theta = 0.47, \beta_u = 0.2, \beta_r = 0.23$.

The HCLPF is defined in terms of individual uncertainties β_R and β_U as

$$A_{HCLPF} = \bar{A} \exp(-1.65\beta_R - 1.65\beta_U) \quad (3)$$

or using a composite uncertainty as

$$A_{HCLPF} = \bar{A} \exp(-2.33\beta_C) \quad (4)$$

where

$$\beta_C = \sqrt{\beta_R^2 + \beta_U^2} \quad (5)$$

Kennedy and Ravindra (1984) present a methodology for estimating the median factor of safety and associated uncertainties using a separation of variables (or fragility method) approach. In this method, the median factor of safety is derived as a product of intermediate factors of safety. Kennedy and Ravindra (1984), EPRI (1994), and Pisharady and Basu (2010) provide information on the calculations.

The separation of variables approach requires the analyst to have knowledge of the median factors of safety of the individual contributors to both seismic demand and capacity, including strength, damping, inelastic energy absorption, spectral shape, and modal combinations. It requires that estimates be made of the underlying randomness and uncertainty in each of the individual factors of safety. Most practicing design engineers however are uncomfortable working in terms of median capacity and response levels, and obtaining or estimating the underlying uncertainties in capacity and demand. Accordingly, an alternate approach to estimating fragilities was developed, which is described as either the Conservative Deterministic Failure Margins (CDFM) approach or the Hybrid approach; EPRI (1991, 1994, 2009, 2013) provide details.

USE OF SEISMIC FRAGILITIES TO ESTIMATE ANNUAL RISK

Seismic fragilities developed using either of the approaches identified above are used in a probabilistic risk assessment to estimate the mean annual frequency of some damage state, which for nuclear power plants can be core damage and for other nuclear structures can be loss of confinement. To calculate the annual frequency of seismic *failure*, the fragility must be convolved with the seismic hazard, namely:

$$P_F = -\int_0^{+\infty} \left(\frac{dH(a)}{da} \right) P_{F|a} da \quad (6)$$

where $P_{F|a}$ is the fragility curve introduced above and $H(a)$ is the seismic hazard curve, which plots the mean annual frequency of exceedance versus a ground motion parameter, which has traditionally been peak ground acceleration but more reasonably could be taken as spectral acceleration at a frequency of significance to the structure, system or component being assessed.

In current practice, the fragility parameters (\bar{A} , β_R , β_U) are set equal to the smallest of the computed values for a component. Consider a flat-bottomed water storage tank. Many of these tanks at the sites of nuclear facilities perform a safety function: condensate storage, refueling water, or demineralized water tanks are examples. The fragility analyst assessing such tanks typically examines common failure modes and considers them to be independent. Table 1 presents typical failure modes for a large flat-bottomed water storage tank, taken from EPRI NP-6041 (EPRI 1991) and BNL-52361 (Bandyopadhyay et al. 1995).

In practice each of these *failure* modes is considered to be independent from each other so that the probability of failure of the tank, $P_f(T)$ is computed by convolving the lowest of the computed fragilities with the hazard using (6). No consideration is typically given to the fact that failure of the tank would result if any failure mode were to occur. More rigorously, the probability of failure should be computed using a systems model, which explicitly considers a combination of failure modes. The systems model represents failure as a Boolean combination of individual events using (*and*, *or*) gates.

Table 1. Seismic failure modes for flat-bottomed storage tanks (EPRI, 1991)

Tag	Failure mode	Consequence of failure
A	Exceed overturning moment capacity	Tearing and/or buckling of shell, leading to loss of contents
B	Exceed sliding capacity	Tearing of attached piping, leading to loss of contents
C	Exceed fluid pressure capacity	Tearing of shell near anchor bolt chair weldments, leading to loss of contents
D	Exceed freeboard	Local damage, loss of content.
E	Geotechnical (liquefaction, slope instability, differential settlement)	Tearing of attached piping, leading to loss of contents

For the example considered here, each failure mode would trigger failure of the tank. The probability of failure of the tank is given by

$$P_f(T) = P_f(A) \cup P_f(B) \cup P_f(C) \cup P_f(D) \cup P_f(E) \quad (7)$$

where \cup is the Boolean union operator. The computation of combined failure probability per (7) is not straightforward because the analyst must consider the correlation of the failure modes. For a system whose failure is controlled by two events, A and B, the system or total probability of failure, $P_f(T)$, is given by:

$$P_f(T) = P_f(A) \cup P_f(B) = P_f(A) + P_f(B) - P(AB) \quad (8)$$

The challenge here is the calculation of the probability of the joint event, $P(AB)$:

$$P(AB) = P(A|B)P(B) \quad (9)$$

where $P(A|B)$ is the (conditional) probability of A given B, which is measured by correlation. For dependent failure modes A and B, this conditional probability is 1.0 and the total probability per (8) becomes:

$$P_f(T) = P_f(A) + P_f(B) - 1 \times P_f(B) = P_f(A)$$

For dependent (or perfectly correlated) failure modes, the fragility function with the smallest median can be used to assess risk (assuming the logarithmic standard deviations are similar). However, it is highly unlikely that two failure modes are either uncorrelated (independent) or fully correlated (dependent) and that there will be some degree of correlation or dependence, namely, the correlation coefficient of two failure modes, A and B, ρ_{AB} , is neither zero nor one.

CASE STUDY

In a recent seismic risk assessment conducted for the Los Alamos National Laboratory, the Boolean combinations of individual failure probabilities given by (8) were considered and the resultant failure probabilities were sometimes significantly greater than that computed using the failure mode with the smallest median fragility, as described next.

Methodology

Assume for the case study that the seismically induced failure of a component is governed by two partially correlated modes. An example of this would be a battery rack whose failure could be due to loss of anchorage or buckling of one of its supporting columns. The failure modes are partially correlated because they are dependent on either ground motion or structural response of the rack. Both the anchorage and the column would have been designed for the same level of earthquake shaking (perhaps a safe shutdown earthquake, SSE) and likely have similar margins to failure if the same materials standard had been used for design and no additional conservatism had been introduced. The failure of the anchorage under tensile loading would increase the probability of brace buckling due to increased loading associated with a change in load path. The individual failure modes would be described using fragility functions, each with a median (50%-ile failure probability) and a logarithmic standard deviation.

Assume the fragility parameters for failure mode 1 are described by a median capacity \bar{A}_1 and a composite uncertainty β_{c_1} , which is given by (5). Similarly, assume the corresponding fragility parameters for failure mode 2 are \bar{A}_2 and β_{c_2} . One measure of how *closely spaced* the modes are in fragility space is given by the ratio of the medians. A value of 1 would indicate identical median capacity. In general, there is one dominant failure mode (smallest median) and this ratio is small. Simulations were performed for \bar{A}_1/\bar{A}_2 between 0.95 and 0.60, and three degrees of correlation, ρ_{12} : 0.90, 0.65 and 0.40.

Ten thousand simulations were generated for each of the failure modes. To ensure that the tails of the distributions were reasonably represented, the simulations were generated as follows: 1) assume a uniformly distributed density function from 0 to 1 to represent the possible space of cumulative probabilities p , and 2) generate m vectors of size n by randomly picking a cumulative probability p from the uniform distribution in step 1 and computing the value of the standard normal variate at that probability. An example is shown in Figure 2 for $m = 2$ vectors with $n = 50$.

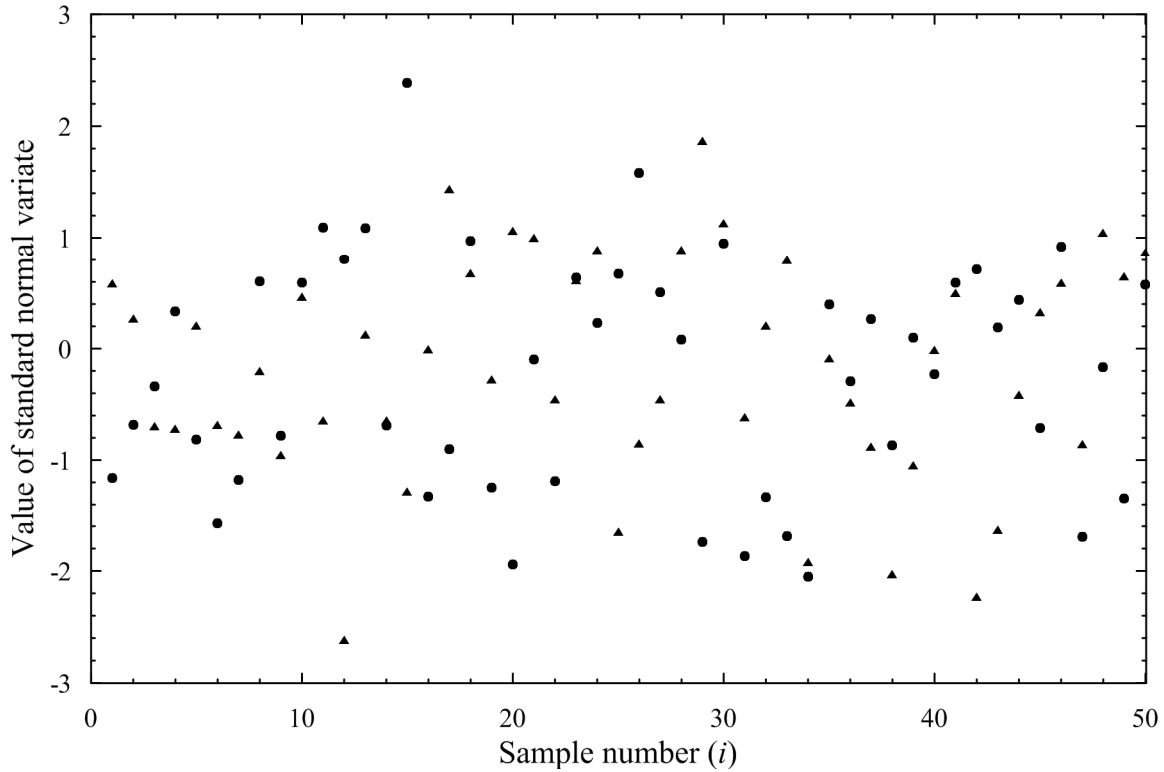


Figure 2. Realizations of the standard normal variate for two samples

The fragility functions can be obtained by back calculating the value of the capacity associated with the standard normal variate:

$$A_{1i} = \bar{A}_1 \exp(S_i \beta_{c1}) \quad (10)$$

where S_i is the value of the standard normal variate and other terms were defined previously. This assumes no correlation between the samples. However, because the failure modes are triggered by the same ground motion, the samples are partially correlated. EPRI 2013 notes that β_c for component fragility is between 0.3 and 0.5, and that a portion of this is due to ground motion. EPRI 1994 assigns $\beta_R = 0.24$ for ground motion. A fraction of the total uncertainty in the fragility model can be assumed to be *dependent* and the remainder *independent*. The *independent* fraction is that variability assigned to capacity and response for dissimilar components (e.g., water storage tanks and battery racks): assumed to be statistically independent for different failure modes. For failure modes of the same component a significant fraction of the uncertainty is dependent (or correlated). The correlation between two failure modes is captured by a) sampling the independent variability as uncorrelated, and b) sampling the dependent variability as perfectly correlated. From 3 sets of n standard variates obtained in step 1, the resulting samples would be obtained as follows:

$$A_{1i} = \bar{A} \exp(S_{1i} \beta_{1I} + S_{2i} \beta_{1D}) \quad (11)$$

and

$$A_{2i} = \bar{A}_2 \exp(S_{3i}\beta_{2I} + S_{2i}\beta_{2D}) \quad (12)$$

where β_{*I} and β_{*D} are the independent and dependent portions of total variability, respectively. The same vector of standard normal variates is used for β_{*D} for generating the samples for A_1 and A_2 . The sample from the Boolean combination, $(A_1 \cup A_2)$, is taken as the minimum of A_{1i} or A_{2i} at each sample point: as given by (12). Figure 3 presents an example of this simulation.

$$A_{co_i} = \min(A_{1i}, A_{2i}) \quad (13)$$

The resulting probability (or annual frequency) of failure can then be computed by convolving (13) with the resulting cumulative density function that best fits the data from the results of the simulations. For this case study, the lognormal distribution fit the data from (13) well. If the dependent and independent portions of the variability differ considerably, the lognormal distribution may not fit the data and the cumulative density function would have to be numerically integrated over the seismic hazard curve.

Results

The assumed parameters for the two partially correlated variables along with the results for the computed total probability of failure, $P_f(T)$, are presented in Tables 2 through 4. Table 2 is for failure modes that have a high degree of correlation ($\rho_{12}=0.90$). Table 3 is for failure modes that are largely uncorrelated ($\rho_{12}=0.40$). Table 4 is for failures modes that have intermediate correlation ($\rho_{12}=0.65$). As expected, the effect of not taking a systems-oriented approach to the risk calculation (i.e., $P_f(1 \cup 2)$) is small for failure modes that are well separated, where $P_f(1 \cup 2)$ is an abbreviation of $P_f(1) \cup P_f(2)$. Other observations from the data presented in these tables include:

- The error introduced by computing the probability of failure based only on the controlling fragility curve (as measured by median capacity) is less than 5% for failure modes that are well separated in fragility space. If the median capacity of the controlling fragility is less than one half of that of the closest neighboring fragility, risk can be calculated using the controlling fragility only with no loss of accuracy regardless of the correlation between the modes.
- The error introduced by computing the probability of failure based only on the controlling fragility curve, if the median values of the fragility curves are similar, is greater if the failure modes are weakly correlated (i.e., $\rho_{12} \leq 0.50$).
- The error introduced by computing the probability of failure based only on the controlling fragility curve is small if the failure modes are strongly correlated.

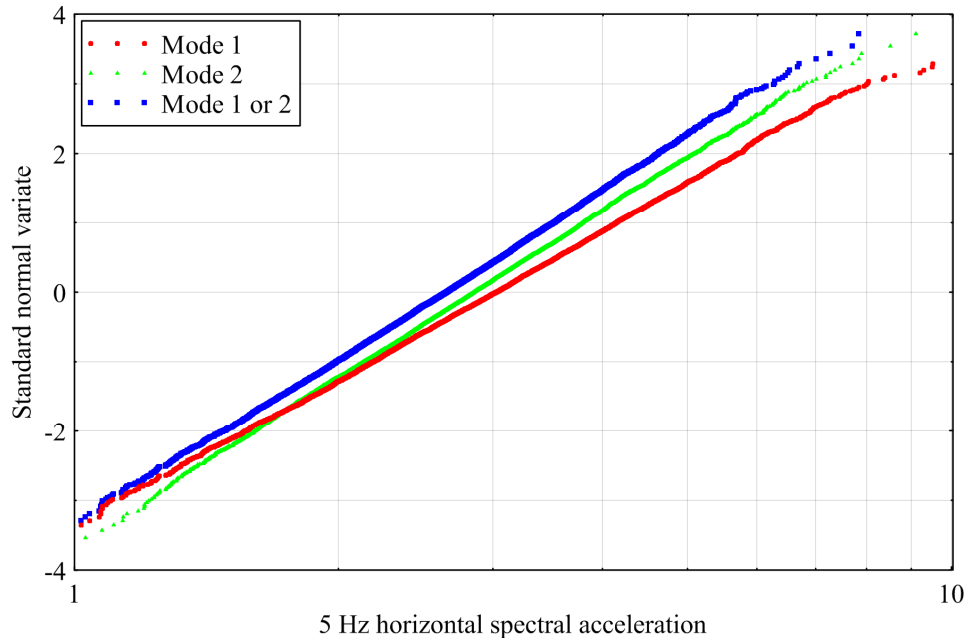


Figure 3. Results of simulations for combined failures

Table 2. Single and combined failure modes with $\rho_{12} = 0.90$ for LANL 5 Hz spectral acceleration and $\beta_{c1} = 0.32, \beta_{11} = 0.12, \beta_{c2} = 0.29, \beta_{12} = 0.06$

\bar{A}_1	\bar{A}_2	$\frac{A_1}{A_2}$	$P_{f1} \times 10^5$	$P_{f2} \times 10^5$	$P_f(1 \cup 2) \times 10^5$	$\frac{P_{f1}}{P_f(1 \cup 2)}$
2.85	3.00	0.95	3.51	3.20	3.84	0.91
2.70	3.00	0.90	4.04	3.20	4.22	0.96
2.55	3.00	0.85	4.67	3.20	4.76	0.98
2.40	3.00	0.80	5.39	3.20	5.47	0.99
2.25	3.00	0.75	6.29	3.20	6.30	1.00
2.10	3.00	0.70	7.41	3.20	7.43	1.00
1.95	3.00	0.65	10.6	3.20	10.6	1.00
1.80	3.00	0.60	15.6	3.20	15.6	1.00

CONCLUSIONS AND RECOMMENDATIONS

A simulation technique was introduced wherein joint probabilities for failure modes that are closely spaced in fragility space can be computed. The use of a controlling fragility function, measured here in terms of lowest median capacity, may under predict component failure rates if that component has closely spaced failure modes (fragility functions), and those failure modes are either uncorrelated or are weakly correlated.

On the basis of the example presented in this paper, a) if the median capacity of the controlling fragility is less than one half of that of the closest neighboring fragility, risk can be calculated using the controlling fragility only with no loss of accuracy, regardless of the correlation between the modes, and b) the error introduced by computing the probability of failure based only on the controlling fragility curve, if the median values of neighboring fragility curves are similar, can be significant if the failure modes are weakly correlated but will be small if the modes are strongly correlated.

More research and case studies are needed to generalize the conclusions made above, including consideration of three or more failure modes per component. Alternate procedures will be needed if fragility functions for a given component utilize different intensity measures (e.g., spectral accelerations at 2 Hz and 0.4 Hz for the impulsive mode [leading to anchorage weldment failure of Table 1] and convective mode [leading to overtopping of the tank wall in Table 1], respectively), requiring nonlinear response-history analysis using appropriately selected and scaled ground motions (e.g., Huang et al. 2011).

Table 3. Single and combined failure modes with $\rho_{12} = 0.40$ for LANL 5 Hz spectral acceleration and $\beta_{c1} = 0.40, \beta_{f1} = 0.30, \beta_{c2} = 0.40, \beta_{f2} = 0.30$

\bar{A}_1	\bar{A}_2	$\frac{A_1}{A_2}$	$P_{f1} \times 10^5$	$P_{f2} \times 10^5$	$P_f(1 \cup 2) \times 10^5$	$\frac{P_{f1}}{P_f(1 \cup 2)}$
2.85	3.00	0.95	4.34	3.79	5.69	0.76
2.70	3.00	0.90	4.92	3.79	6.13	0.80
2.55	3.00	0.85	5.65	3.79	6.70	0.84
2.40	3.00	0.80	6.47	3.79	7.31	0.89
2.25	3.00	0.75	7.52	3.79	8.24	0.91
2.10	3.00	0.70	8.81	3.79	9.39	0.94
1.95	3.00	0.65	10.4	3.79	10.8	0.96
1.80	3.00	0.60	12.4	3.79	12.7	0.98

Table 4. Single and combined failure modes with $\rho_{12} = 0.65$ for LANL 5 Hz spectral acceleration and $\beta_{c1} = 0.32, \beta_{f1} = 0.20, \beta_{c2} = 0.29, \beta_{f2} = 0.15$

\bar{A}_1	\bar{A}_2	$\frac{A_1}{A_2}$	$P_{f1} \times 10^5$	$P_{f2} \times 10^5$	$P_f(1 \cup 2) \times 10^5$	$\frac{P_{f1}}{P_f(1 \cup 2)}$
2.85	3.00	0.95	3.49	3.22	4.20	0.83
2.70	3.00	0.90	4.21	3.22	4.72	0.89
2.55	3.00	0.85	4.84	3.22	5.23	0.92
2.40	3.00	0.80	5.63	3.22	5.89	0.96
2.25	3.00	0.75	6.55	3.22	6.70	0.98
2.10	3.00	0.70	7.74	3.22	7.81	0.99
1.95	3.00	0.65	9.13	3.22	9.15	1.00
1.80	3.00	0.60	10.6	3.22	10.6	1.00

REFERENCES

- American Society of Civil Engineers (ASCE). 2000. "Seismic analysis of safety-related nuclear structures and commentary." *ASCE 4-98*, Reston, VA.
- American Society of Civil Engineers (ASCE). 2005. "Seismic design criteria for structures, systems and components in nuclear facilities." *ASCE 43-05*, Reston, VA.
- American Society of Mechanical Engineers (ASME). 2013. "Standard for level 1/large early release frequency probabilistic risk assessment for nuclear power plant applications." *ASME/ANS RA-Sb-2013*, New York, NY.
- Bandyopadhyay, K., A. Cornell, C. Costantino, R. P. Kennedy, C. Miller, and A. Veletsos. 1995. "Seismic design and evaluation guidelines for the Department of Energy high-level waste storage tanks and appurtenances." *BNL 52361*, Brookhaven National Laboratory, NY.
- Electric Power Research Institute (EPRI). 1991. "A methodology for assessment of nuclear power plant seismic margin (Revision 1)." *EPRI-NP-6041-SL*, Palo Alto, CA.
- Electric Power Research Institute (EPRI). 1994. "A methodology for developing seismic fragilities." *EPRI TR-103959*, Palo Alto, CA.
- Electric Power Research Institute (EPRI). 2009. "Seismic fragility applications guide update." *EPRI TR-1019200*, Palo Alto, CA.
- Electric Power Research Institute (EPRI). 2013. "Seismic evaluation guidance, screening, prioritization and implementation details (SPID) for the resolution of Fukushima Near-Term Task Force recommendation 2.1: seismic." *EPRI 1025287*, Palo Alto, CA.
- Huang, Y.-N., A. S. Whittaker, and N. Luco. 2011. "A seismic risk assessment procedure for nuclear power plants, (I) methodology." *Nuclear Engineering and Design*, Vol. 241, pp. 3996-4003.
- Kennedy, R. P. and M. K. Ravindra. 1984. "Seismic fragilities for nuclear power plant risk studies." *Nuclear Engineering and Design*, Vol. 79 (1), pp. 47-68.
- Pisharady, A. S. and P. Basu. 2010. "Methods to derive seismic fragilities of NPP components: a summary." *Nuclear Engineering and Design*, Vol. 240, pp. 3878-3887.